Journal of Cleaner Production 362 (2022) 132447

Contents lists available at ScienceDirect

Journal of Cleaner Production

journal homepage: www.elsevier.com/locate/jclepro

Shock loads change the resistance, resiliency, and productivity of anaerobic co-digestion of municipal sludge and fats, oils, and greases

Ashley E. Berninghaus, Tyler S. Radniecki *

School of Chemical, Biological, and Environmental Engineering, Oregon State University, Corvallis, OR, 97331, USA

ARTICLE INFO

Handling Editor: Zhen Leng

Keywords:
Anaerobic co-digestion
FOG
Perturbation
mcrA
Resilience

ABSTRACT

Accidental organic overloading (shock loading) is a common cause of failure in the anaerobic co-digestion of fats, oils, and greases (FOG). Nonetheless, questions still remain about how shock loads alter an anaerobic digester's biogas productivity and response to future organic overloads. To address this knowledge gap, this study utilized short increases in OLR, or shock loads, to adapt one reactor to FOG co-digestion and compare its response to that of a non-adapted digester tested at similar organic loads. A long-term study was also conducted where sequential shock events and disturbance-to-failure events (with organic loading rates ranging from 2.5 to 9.0 g VS/L/d) were employed to study their effects on reactor stability and performance. When exposed to moderate and large shock loads (3.0 and 9.0 g VS/L/d, respectively), the anaerobic digester previously exposed to FOG shock loads had greater levels of resistance and resiliency. For a moderate shock, it took the non-adapted reactor 29.8, 43, 44, and 19 days longer than the adapted reactor to recover to the baseline levels for methane content, organic acids (OA), pH, and *mcrA* concentrations, respectively. For a large shock, the adapted and non-adapted reactors saw more similar recovery times with the non-adapted reactor requiring an additional 11, 18, 19, and 0 days longer than the adapted reactor to recover to baseline levels for methane content, OA, pH, and *mcrA* concentrations, respectively. However, exposure to successive large shock loads decreased the anaerobic digester's resistance and resilience. The length of time it took for the organic acid accumulation and methane content values to return to their pre-shock values generally increased with each successive large shock load. For OA, the reactor required 35, 39, and 43 days to recover from the first, second, and third large shocks, respectively, while the methane content recovery times were 27.5, 26.5, and 34.5 days for the same shock periods. Thus, this work demonstrates that there is a tipping point in which FOG shock loads, whether intentional or accidental, go from improving the overall robustness of an anaerobic digester to significantly deteriorating its overall performance.

1. Introduction

Recently, a focus has been placed on the natural production of methane via anaerobic digestion and its place in the water-energy-food nexus. This is due to its ability to digest organic matter (food waste) and produce methane, a renewable energy source (Lee et al., 2021; Parry, 2010). The anaerobic co-digestion of energy-rich fats, oils, and greases (FOG) has been recognized as an effective, low-cost, and commercially viable approach to improve methane yields to levels needed to encourage energy recovery efforts at wastewater treatment facilities (Grosser and Neczaj, 2018; Li et al., 2013). Studies have shown that FOG has a methane yield potential per gram volatile solids (VS) that is 250%–350% greater than wastewater sludge itself (Ziels et al., 2016). Despite reported benefits of co-digestion, efforts to intensify the FOG co-digestion process and increase its predictability to process changes have been hampered by a limited fundamental understanding of how the anaerobic digester microbiome responds to process disturbances, such as a change in substrate or loading rate (Salama et al., 2019).

Previous studies have evaluated a wide range of organic loading rates (OLRs), ranging from 0.05 to 7.47 g VS/L/d, resulting in methane yields from 200 to 600 mL methane/g VS (Davidsson et al., 2008; Kabouris et al., 2008; Luostarinen et al., 2009; Wang et al., 2020). However, to date, no general conclusions about the limits of FOG co-digestion (i.e. the threshold loading rate at which FOG co-digestion causes failure) can be drawn from these empirically derived results. For example, where some studies have observed failure at 1.45, 2.5, 4.0, and 7.47 g VS/L/d, other studies have shown an ability to operate between 1.3 and 3.0 g VS/L/d without upset (Wang et al., 2020). This wide range of results demonstrates that the productivity and stability of FOG

* Corresponding author. 105 SW 26 th St, Corvallis, OR, 97331, USA.
E-mail address: tyler.radniecki@oregonstate.edu (T.S. Radniecki).

https://doi.org/10.1016/j.jclepro.2022.132447
Received 24 September 2021; Received in revised form 5 April 2022; Accepted 26 May 2022
Available online 31 May 2022

Nomenclature

COD	Chemical Oxygen Demand
DNA	Deoxyribonucleic Acid
FOG	Fats, Oils, and Greases
HPLC	High Performance Liquid Chromatography
HRT	Hydraulic Retention Time
OA	Organic Acid
OLR	Organic Loading Rate
LCFAs	Long-chain Fatty Acids
qPCR	Quantitative Polymerase Chain Reaction
RAS	Recycled Activated Sludge
SRT	Solids Retention Time
TAN	Total Ammonia Nitrogen
TS	Total Solids
TWAS	Thickened Waste Activated Sludge
VS	Volatile Solids

co-digestion is highly dependent upon FOG composition, loading rate, and microbial community adaptation and the interactions between these three parameters, as opposed to one being deterministic of reactor response on its own (Long et al., 2012; Salama et al., 2019; Suto et al., 2006).

In order to draw conclusions about FOG addition and to optimize the process, these empirical results need to be paired with microbial indicators of optimal performance to develop microbial management strategies (Carballa et al., 2015). One of the most popular ways to link the microbial community to digester performance is through the use of alternative feeding strategies, such as changes in OLR, v/v ratio of substrates, or feeding frequency (Carballa et al., 2015; Goux et al., 2015; Luostarinen et al., 2009; Ziels et al., 2017). Two studies have specifically demonstrated microbial community adaptation and improved reactor performance while performing co-digestion of FOG via step-loading (Silvestre et al., 2011) and using pulse-feeding of long-chain fatty acids (LCFAs) (Kougias et al., 2016). However, these studies were relatively short-term disturbances and did not examine process failure or post-failure recovery and the potential microbial community adaption that ensued. Two recent studies have focused on comparing an adapted and a non-adapted digester's response to a disturbance (Deaver et al., 2021; Wang et al., 2020). The first only evaluated a gradual increase in OLR, also known as step-loading, or a press disturbance, with fairly long disturbance periods (ranging between 20 and 80 days in length) (Wang et al., 2020). The second only assessed one disturbance event and its effect on the microbial community, but did not then evaluate how that disturbance event affected the reactor's resilience. Although both were able to provide a more direct comparison of how compositional differences in the microbiome can lead to functional differences, they still do not aid in the understanding of repeated short-term disturbance events.

A step-loading regime, or press disturbance, is one of two commonly identified options to directly alter a community (Shade et al., 2012). The other option is a pulse disturbance, which is defined as a relatively discrete, short-term event as compared to a press disturbance which is a long-term or continuous disturbance (Shade et al., 2012). To the authors' knowledge, there are no other studies that have used shock loading of FOG, or pulse disturbances, to study the effects on the microbial community composition. These types of disturbances may provide another option for microbial community adaptation to FOG co-digestion as well as providing insight into what might happen when accidental overfeeding events happen due to changes in substrate composition or a lack of mixing in a FOG storage vessel.

To address this knowledge gap, this study utilized short increases in OLR, or shock loadings, to adapt one reactor to FOG co-digestion and its response was compared to a non-adapted reactor tested at similar organic loads. A long-term study was also conducted where the effects of sequential shock events, which utilized shocks that resulted in a disturbance-to-failure experience and those that did not result in failure, and their effects on reactor stability and performance. Post-failure recovery was compared for a variety of operational parameters, including *mcrA* quantification, to understand how the microbiome functionality was affected by shock events. Quantification of the extent and magnitude of the reactor response was performed using a resilience model proposed by Todman et al. to better explain post-failure recovery periods (Todman et al., 2016).

2. Materials and methods

2.1. Seed anaerobic digestate and FOG source

Seed anaerobic digestate was collected from a full-scale mesophilic anaerobic digester at the City of Corvallis Wastewater Reclamation Plant (Corvallis, OR). The anaerobic digester receives only municipal sludge and operates at a 30 d solids retention time (SRT). Recycled activated sludge (RAS) was also acquired from the Corvallis Wastewater Reclamation Plant and was sampled directly from the RAS pipeline. FOG was collected from the FOG receiving station at the City of Gresham Wastewater Reclamation Plant (Gresham, OR) and contained a mixture of grease trap waste from restaurants, fast food, and commercial kitchens, as well as fat from a milk processing plant in the greater Portland, OR area. The FOG had a total solids (TS) and volatile solids (VS) content of 101.1 ± 1.6 g TS/L and 98.3 ± 1.6 g VS/L, respectively, resulting in an average VS/TS ratio of 0.97 ± 0.00 g VS/g TS.

Continuously stirred tank reactors were inoculated with anaerobic digestate within 1 h of its collection. The RAS was thickened to five times the original VS content via centrifugation at 5000 rpm for 10 min (final VS content was approximately 17 g/L). The thickened RAS and collected FOG were stored at 4 °C prior to their use. To achieve higher OLRs during FOG shock events, the FOG was dewatered. This was achieved by allowing the FOG to settle and separate via gravity for 4 h at room temperature, at which point the aqueous phase was removed. To further thicken the FOG, it was submerged in a 50 °C water bath for 10 min before being cooled at room temperature for 6 h, at which point the aqueous phase was removed.

2.2. Experimental set-up

2.2.1. Long-term shock study

The long-term shock study was carried out in a continuously stirred tank reactor with a working volume of 1.5 L and an operating temperature of 37 °C. The reactor was equipped with a liquid sampling port, a gas sampling port, and a baffled, magnetic stir bar (Fig. 1). The reactor was mixed at approximately 60 rpm during the experiment. Immediately following inoculation with the Corvallis anaerobic digestate, the reactor was sparged with N_2 for 30 min to ensure that the headspace was anaerobic.

The reactor was run for a total of 335 days divided into shock and recovery phases in order to study the effect of digester productivity following successive high OLR shock events (Table 1). During the initial baseline phases (30 d and 15 d HRT), only RAS was fed to the reactor. Following the baseline phases, the reactor saw two different modes of operation throughout the duration of the experiment. Shock periods were defined as high organic load periods where a mixture of RAS and FOG was fed while recovery periods were defined as low organic load periods where only RAS was fed.

Shocks were administered eleven separate times at three different organic loads. Shock A was administered twice with a mixture of RAS and FOG, 1:1 (v/v), which was the lowest organic load tested. Shock B was administered six times with a mixture of RAS and FOG 3:7 (v/v), which was the second largest organic load tested. Shock C was administered three times with a mixture of RAS and thickened FOG, 1:4 (v/v

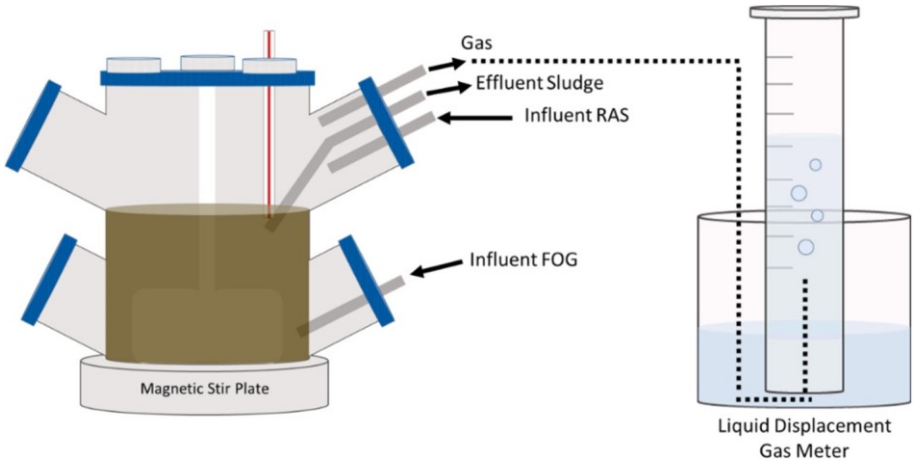

Fig. 1. A schematic of the reactor plumbing and the liquid displacement gas metering system used throughout both long-term and single shock experiments.

%), resulting in the largest organic load tested. After each shock period ended, the reactor went into recovery mode until organic acid levels returned to the range observed during the baseline phase (<50 mg/L) and gas production stabilized.

The ratios for the small and moderate shock loads were chosen in order to achieve OLR values that mimicked the values measured at full-scale FOG co-digestion facilities in the local area. These facilities have OLR values that range from 2.44 to 3.24 g VS/L/d. The ratio for the large shocks was increased, and the FOG was dewatered, in order to achieve an OLR that would induce a failure event.

The HRT remained constant through all shock and recovery periods. No sediment build up was observed at the end of the experiment so the working volumes of the reactor was not corrected. The OLR for each phase is based on the VS content of daily influent samples using Equation (1).

$$OLR = \frac{Influent\ Flow\ Rate, \frac{L}{d}\ x\ Influent\ VS\ Content, \frac{g\ VS}{L}}{Reactor\ Volume, L} \quad \text{Equation 1}$$

2.2.2. Single shock study

The single shock studies were carried out in two continuously stirred tank reactors, A and B. Reactor design and set-up was previously described in section 2.2.1. Both reactors were run side-by-side for 100 days. Both reactors started with an initial baseline phase (30 d and 15 d HRT), where only RAS was fed. Following the baseline phases, Reactor A saw a single C shock (a 1:4 (v/v) RAS:FOG mixture), while Reactor B saw a single B shock (a 3:7 (v/v) RAS:FOG mixture). Following these single shock events, both reactors were fed only RAS during the recovery phase. Table 2 shows an overview of the operational parameters during each phase of the experiment.

2.3. Analytical methods

Volumetric gas production was measured using a liquid displacement gas metering system with water displacement assumed to be equal to volumetric gas production (Fig. 1). An aliquot of the reactor biogas was taken from the reactor's gas sampling port using a glass, gas-tight syringe. Methane content was determined using an HP-5890 GC thermal conductivity detector with argon carrier gas at a flow rate of 20 mL/min with a packed column (Supelco 15' x 1/8" SS support 60/80 Carboxen 1000). The method was isothermal at 220 °C.

Reactor influent and effluent samples were taken daily Monday through Friday. Influent samples were taken from the bottle attached to the influent pump. Effluent samples were taken by collecting the pumped effluent. The following analytes were determined for both the influent and effluent: pH, conductivity, dissolved ortho-phosphate, dissolved total ammonia nitrogen (TAN), TS, and VS. Organic acid (OA) concentrations were only measured on effluent samples.

TS and VS were determined according to EPA Method 1684 (U.S. EPA: Office of Water, 2001). The pH of homogenous sludge samples was measured using a Thermo Orion 9156BNWP pH meter. The conductivity of homogenous sludge samples was measured using a VWR conductivity probe (89231–618). The homogenous sludge was then centrifuged for 5 min at 13,000 rpm. The supernatant was stored at—20 °C prior to further analysis for dissolved TAN, dissolved ortho-phosphate, and OA concentrations.

Dissolved TAN concentrations were measured using a 2-phenylphenol method previously described (Rhine et al., 1998). This assay was modified for use in a 96-well plate as described: 25 μL of sample was combined with 175 μL of citrate reagent, 50 μL of 2-phenylphenol nitroprusside reagent, and 25 μL of buffered hypochlorite. The plate was placed into a BioTek Synergy 2 microplate reader, incubated at 37 °C for 15 min, shaken for 30 s, and absorbance was read at 660 nm.

Dissolved ortho-phosphate was measured using a previously described ascorbic acid colorimetric assay (U.S. EPA, 1978). The assay was modified for use in a 96-well plate as described: 200 μL of sample was combined with 10 μL of 11N sulfuric acid, 40 μL of ammonium molybdate-antimony potassium tartrate reagent, and 20 μL of ascorbic acid reagent. The plate was placed into a BioTek Synergy 2 microplate reader, shaken for 3 m, and absorbance was read at 650 nm.

OA concentrations were determined using a Dionex 500X high performance liquid chromatograph (HPLC) equipped with an AD20 UV absorbance detector, a HiChrom Prevail 5 μm organic acid column (250 × 4.6 mm). The HPLC ran in isocratic mode for 35 min per sample with a 0.06 M phosphate eluent at a flowrate of 1 mL/min for the first 8 min follow by a 1.5 mL/min flowrate for the following 27 min. Absorbance was measured at 210 nm.

2.4. DNA extraction

DNA was extracted from aliquots of sludge throughout each experiment (44 samples total for the long-term experiment and 12 samples total for each of the short-term experiments). For each sample, DNA was extracted from 500 μL of homogenous anaerobic digestate sludge. Prior to extraction, each anaerobic digestate sample was washed with a 1 mM sodium bicarbonate solution three times. Washed homogenous sludge was then dewatered via centrifugation (11,000 rpm for 1 min) and DNA was extracted using the Qiagen DNeasy PowerSoil DNA Extraction Kit (Qiagen, Venlo, Netherlands) according to manufacturer instructions. Total DNA concentration and quality was quantified using a NanoDrop One (Thermo Fisher Scientific, Waltham, MA, USA). The DNA was further cleaned and concentrated using a Monarch PCR and DNA

Table 1
Overview of process parameters during the long-term experiment. Values presented are the average values over each operational phase. Numbers in brackets represent 95% confidence intervals.

Parameter	Unit	Baseline		Shock A		Shock B					Shock C			Recovery
		30 d HRT (0–26)	15 d HRT (26–46)	1 (46–50)	2 (72–81)	1 (95–105)	2 (116–126)	3 (137–147)	4 (195–207)	5 (246–256)	6 (316–327)	1 (158–161)	2 (207–210)	3 (270–273)	(Between shocks)
HRT	Days	30	15	15	15	15	15	15	15	15	15	15	15	15	15
Temp.	°C	37	37	37	37	37	37	37	37	37	37	37	37	37	37
RAS Feed	L/d	0.05	0.1	0.05	0.05	0.03	0.03	0.03	0.03	0.03	0.03	0.02	0.02	0.02	0.1
FOG Feed	L/d	0	0	0.05	0.05	0.07	0.07	0.07	0.07	0.07	0.07	0.08	0.08	0.08	0
OLR	g VS/(L·d)	0.72 [0.07]	1.14 [0.11]	3.02 [0.74]	2.21 [0.54]	2.87 [0.28]	3.08 [0.06]	3.23 [0.21]	3.44 [0.12]	3.36 [0.45]	3.54 [0.11]	10.71 [1.62]	8.77 [0.45]	8.78 [0.56]	1.08 [0.04]

Cleanup Kit (New England Biolabs, Ipswich, MA, USA).

2.5. Quantitative polymerase chain reaction (qPCR)

qPCR was performed in triplicate according to the protocol established by Morris and colleagues (Morris et al., 2014), using the primers designed by Luton and colleagues (Luton et al., 2002). The final qPCR mix per 20 μL reaction was as follows: 1X SsoAdvanced Universal SYBR Green Supermix (Bio-Rad Laboratories, Hercules, CA, USA), template DNA (0.2 – 1 ng), 750 nM mcrF and mcrR, and nuclease-free water to bring the final reaction volume up to 20 μL. Each qPCR run included a no-template control and was performed in the Bio-Rad CFX Connect Real-Time PCR Detection System (Bio-Rad Laboratories, Hercules, CA, USA) using the following program: initial denaturation at 95 °C for 10 min, 45 cycles of 95 °C for 30 s and 58.5 °C for 1 min, and a final extension of 7 min at 72 °C, followed by a melt curve to check for product specificity. Starting quantity amounts and threshold cycle values were calculated using the accompanying Bio-Rad CFX Manager software.

qPCR standards used in all runs were created using pooled *mcrA* clones (Integrated DNA Technologies, Coralville, IA, USA). Five clones were chosen from the accession numbers from Morris and colleagues (Morris et al., 2014). Their nucleotide sequences can be found in GenBank® under accession numbers HM800534, HM800536, HM800549, HM800574, and HM800611.

2.6. Resilience model

The resilience model proposed by Todman et al. is based off of an analogy with a mechanical spring and damper system, was used to quantify reactor recovery response rates. This model identifies four separate characteristics of reactor recovery as such: the degree of return (R_r), the return time (R_t), the rate of return (R_r), and the "efficiency" of the return (R_e) (Todman et al., 2016). Due to the nature of the system studied, the model proposed by Todman et al. did not provide sufficient fits to determine the four terms identified so modifications were made to apply the model concepts. The degree of return was treated as a binary option to determine if the system did or did not recover to pre-shock levels. The rate of return was determined manually based on when the recovery response was equal to the pre-shock value. The "efficiency" was calculated as the area under the curve using the AUC function in R. For this study, it was determined that the rate of return was not a parameter of concern.

3. Results and discussion

3.1. Nutrient concentrations and volatile solids measurements

Nutrient concentrations were measured throughout the long-term and single shock experiments in both the influent and effluent (Figs. S2 and S4). Both dissolved ammonium and dissolved phosphorous generally increased with increased OLR and with the presence of FOG. While ammonia toxicity can be problematic in anaerobic digestion, the total ammonia concentrations observed stayed below the identified toxicity thresholds which range from 1500 to 5000 mg/L total ammonia nitrogen (Wang et al., 2016; Yenigun and Demirel, 2013). When the measured nutrient concentrations were normalized to the influent VS, the normalized values were generally consistent (average values were 83.49 ± 3.52 mg N/g VS and 14.43 ± 0.38 mg P/g VS) (Figs. S2 and S4). Influent and effluent VS measurements were also determined throughout the duration of the long-term and single-shock experiments. These data show that the VS content of the digester generally increased with increased OLR. During periods of co-digestion, higher VS reduction efficiencies were achieved compared to RAS only phases (average during A and B shocks was 75.1 ± 2.2% while neighboring RAS only phases averaged 42.4 ± 3.5%) (Figs. S2 and S4). However, the C-shocks

Table 2
Overview of process parameters during both single shock experiments. Values presented are the average values over each operational phase. Numbers in brackets represent 95% confidence intervals.

Parameter	Unit	Reactor A				Reactor B			
		Baseline		C Shock	Recovery	Baseline		B Shock	Recovery
		30 d HRT (0–14)	15 d HRT (14–32)	(32–35)	(35–100)	30d HRT (0–14)	15d HRT (14–38)	(38–48)	(48–100)
HRT	Days	30	15	15	15	30	15	15	15
Temp.	°C	37	37	37	37	37	37	37	37
RAS Feed	L/d	0.05	0.1	0.02	0.1	0.05	0.1	0.03	0.1
FOG Feed	L/d	0	0	0.08	0	0	0	0.07	0
OLR	g VS/(L·d)	0.48 [0.03]	1.19 [0.16]	9.94 [0.71]	1.02 [0.05]	0.48 [0.03]	1.09 [0.17]	3.26 [0.39]	0.95 [0.05]

resulted in large build-ups of residual VS (up to 22.1 g VS/L effluent) and, consequently, negative VS reduction efficiencies (the lowest recorded value was —131%).

3.2. Efficacy of pre-exposure to FOG for improving reactor resilience

Single-shock experiments were used to establish a baseline response, in terms of reactor productivity and stability, after an initial exposure to moderate and high FOG loading rates. One reactor experienced a single moderate B-shock with an OLR of 3.27 g VS/L/d. A second reactor experienced a single large C-shock with an OLR of 9.94 g VS/L/d. In order to better understand the efficacy of pre-exposure in mitigating reactor upset during FOG co-digestion, these baseline responses were compared to a third reactor which was adapted to FOG through a series of small A-shocks (OLR of 2.53±0.49 g VS/L/d) prior to experiencing repeated B-shocks and C-shocks.

3.2.1. Initial adaptation phase of the adapted reactor

The adaptation of the adapted reactor started with an accidental organic overload of TWAS due to a clogged pump during the 15 d HRT phase. This did result in a moderate upset in terms of methane content (decreased to 60%) and organic acid accumulation (peak total OA accumulation of 2.28 g/L) (Fig. 2D and E). Although the organic overload was not due to FOG addition, it should be acknowledged as a possible disturbance that may have resulted in community adaptation.

Following this event, FOG was introduced with two small A-shocks, A1 and A2, (OLR of 2.53 ± 0.49 g VS/L/d) which resulted in increased biogas and methane production rates (Fig. 2B and C). Compared to the preceding TWAS-only phase, biogas production increased 106% (524 ± 84 to 1081 ± 91 mL/d) during A1 and 198% (524 ± 84 to 1563 ± 163 mL/d) during A2. Additionally, the biogas yields were 375 ±63 and 852 ± 293 mL/d for shocks A1 and A2, respectively, while the methane yields were 229±6 and 589 ±105 mL/d for the same shocks. Following the A-shocks, the adapted reactor experienced a series of moderate B-shocks (3.27 ±0.11 g VS/L/d) which resulted in no signs of reactor upset (Fig. 2).

3.2.2. Comparison of the adapted and non-adapted response to a moderate shock (B-shock)

When exposed to a similar moderate shock load, or a B-shock, (OLR of 3.27 ± 0.40 g VS/L/d) the adapted reactor saw a 346% increase in biogas production compared to the preceding TWAS only phase (557 ± 58 to 2484 ±173 mL/L/d), while the non-adapted reactor saw an initial increase in biogas production of 130% during the first 4 days of the shock (310 ± 34 to 712 ± 136 mL/L/d) after which the gas production decreased to approximately 0 mL/L/d for 3 days (Fig. 2B). The methane productivity and methane yield followed the same trends as the biogas for each reactor, respectively (Figs. 3C and 2D).

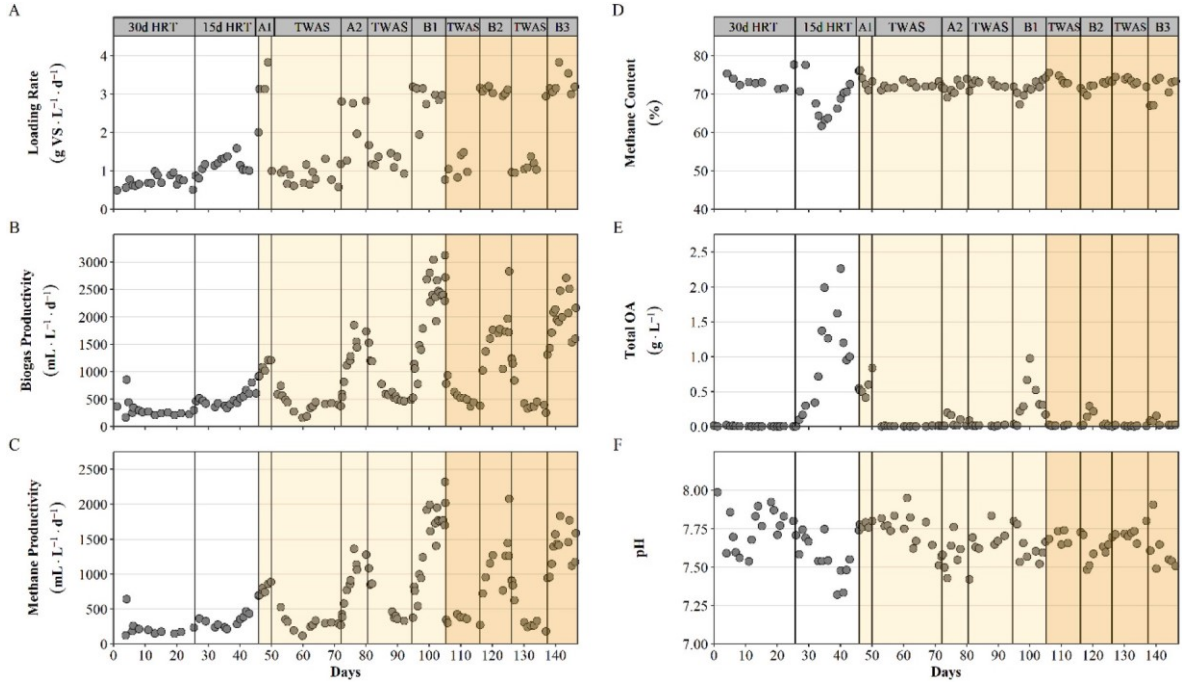

Fig. 2. A) Organic loading rate (OLR), B) biogas production, C) methane production, D) methane content, E) total OA content, and F) pH for days 0–150 of the long-term experiment. The adaptation phase for comparison with a moderate shock is shown in light yellow. The adaptation phase for comparison with a large shock is shown in dark yellow. Black vertical lines designate the different phases of operation.

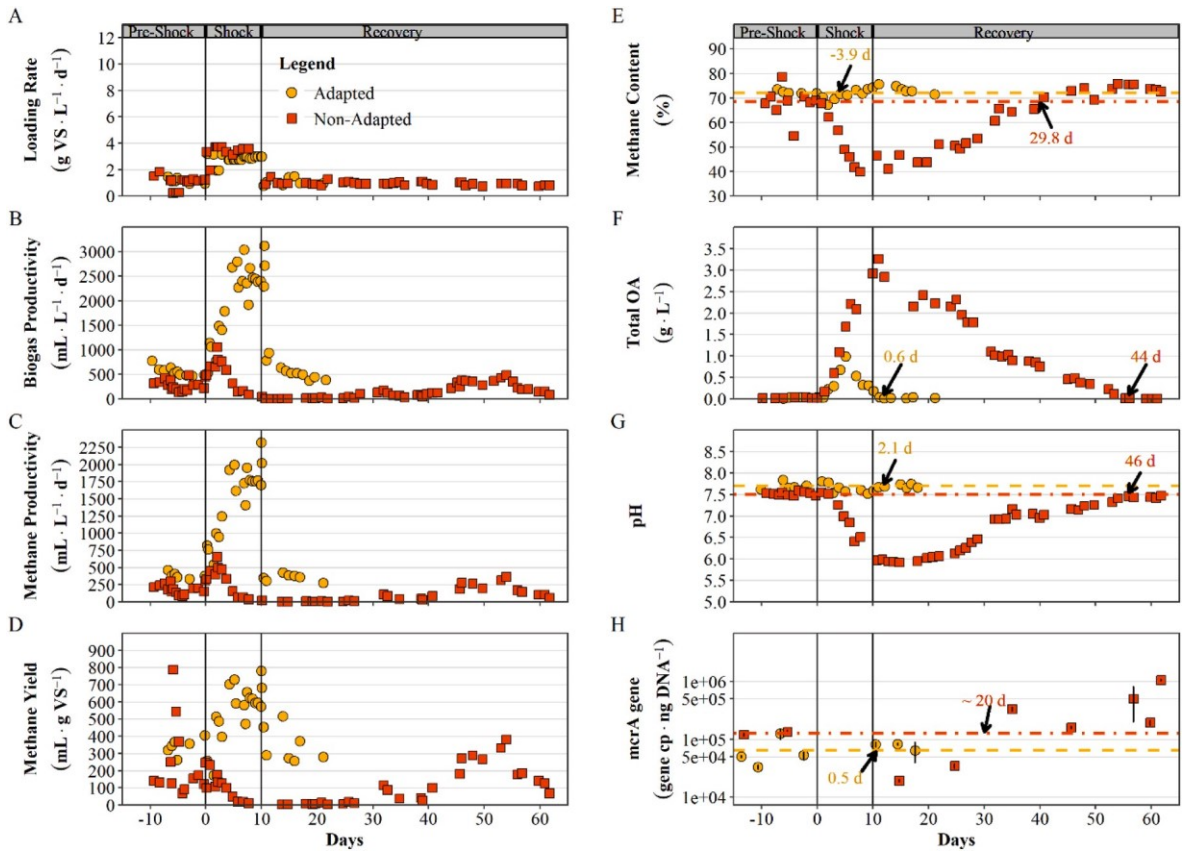

Fig. 3. A) Organic loading rate (OLR), B) biogas production, C) methane production, D) methane yield, E) methane content, F) total OA content, G) pH, and H) *mcrA* quantification for the adapted and non-adapted digesters during the pre-shock, moderate B shock, and recovery phases. Dashed lines represent the pre-shock averages of each respective parameter. Arrows and labeled number of days represent how many days of TWAS only recovery was needed to r each pre-shock levels. Error bars on *mcrA* data represent 95% confidence intervals for triplicate samples.

The methane content in the adapted reactor did not decrease drastically, reaching a low of only 67.2% compared to a pre-shock level of 73% and recovered during the 10-day shock period (Fig. 3E). In comparison, the non-adapted reactor showed signs of methanogen inhibition as the methane content dropped 28% from the pre-shock level of 68% and required 30 days of recovery (TWAS only influent) to return to pre-shock levels (Fig. 3E).

Other parameters measured showed similar trends. Total OA concentrations were 3-times greater in the non-adapted reactor than in the adapted reactor, with peak acetate, propionate, and butyrate concentrations of 1.91 g/L, 0.84 g/L, and 0.71 g/L, respectively, compared to the peak concentrations of 0.93 g/L, 0.05 g/L, and 0 g/L in the adapted reactor (Figs. S1 and S3). A recovery threshold was established where all three OA concentrations had to be below 50 mg/L in order for the system to be considered fully recovered. The adapted reactor met this threshold on the first day of the recovery phase (TWAS only influent), while the non-adapted reactor required 44 days (Fig. 3F).

The pH of the adapted reactor decreased slightly from 7.65 to 7.52 due to the shock (Fig. 3G), but stayed within the ideal range for methanogenic activity of 6.5–8 (Kundu et al., 2017). Meanwhile, the non-adapted reactor saw a dramatic decrease in pH, reaching a low of 5.91, during the shock phase which remained below 6.5 for 22 days and required 46 days of recovery (TWAS only influent) to reach pre-shock levels (Fig. 3G).

Quantification of the *mcrA* gene also indicated that the non-adapted reactor experienced a significant decrease in methanogens, while the adapted reactor did not (Fig. 3H). The methanogen concentration immediately following the shock phase was similar in the adapted reactor to its pre-shock levels. The non-adapted reactor saw a 14% decrease immediately following the shock and returned to pre-shock quantities after about 20 days of recovery (TWAS only influent).

As is common in anaerobic digestion systems, OA accumulation is typically linked with other signs of failure including decreased methane content and decreased pH values. Here, the OA accumulation appears to be the main driver of decreased reactor performance as methane content and *mcrA* gene quantities both did not recover until OA levels fell below 1 g/L. Additionally, pH values did not recover until slightly after the accumulated OAs had been degraded.

For a moderate shock, pre-exposure to FOG promoted adaptation of the anaerobic digester and was the key differentiator between reactor stability and failure (low gas production, high OA accumulation, and inhibition of methanogens). Similar results were observed in a study that employed a press disturbance to adapt and test anaerobic digesters (Wang et al., 2020). In that study, the non-adapted reactor saw a decrease in biogas production and methane yield to almost zero while the methane content decreased from roughly 70% to almost 40% which was similar to the results observed in the present study after applying a moderate shock to the adapted and non-adapted reactor (Fig. 3). Similarly, OA accumulation was observed above 2 g/L and the pH decreased below 6.5 due to the press disturbance (Wang et al., 2020). The moderate shock employed in the present study had a greater OLR than that used by Wang et al. and resulted in a greater accumulation of OA (up to almost 3.5 g/L) and a greater decrease in the pH (5.91 at its lowest).

3.2.3. Comparison of the adapted and non-adapted response to a large shock (C-shock)

In order to determine the efficacy of adaptation for mitigation of reactor failure in the case of a large C-shock (OLR 9.36 ± 0.75 g VS/L/

d), a similar comparison was established. One reactor experienced a single C-shock with no pre-exposure to FOG, while the long-term reactor had seen 5 separate instances of FOG before the large C-shock. As previously described, the long-term reactor received two A-shocks before a B-shock was implemented. Following the first B-shock, two others were implemented in succession with 10 day TWAS only recovery periods in between (Fig. 2A). Generally, these B-shocks resulted in a 362% increase in methane productivity (335 mL CH_4/L/d to 1549 mL CH_4/L/d) compared to the neighboring TWAS only periods (Fig. 2C).

These additional pre-exposure events did help to mitigate some of the effects of the large C-shock, however both the adapted and non-adapted reactors experienced upset. Both reactors demonstrated a slight increase in biogas production during the first day of the shock (214% for the adapted and 141% for the non-adapted). After this initial increase, both reactors saw a rapid decrease in biogas and methane production, with a minimum rate of methane production of 3 mL CH_4/L/d in the non-adapted reactor and 14 mL CH_4/L/d in the adapted reactor (Fig. 4B and 4C). Methane content also decreased drastically, however, the non-adapted reactor fared worse. The adapted reactor reached a low of 45.4% following the shock event, and took 24.7 days of recovery (TWAS only influent) to return to its pre-shock level of 73.6% (Fig. 4E). In comparison, the non-adapted reactor saw a decrease down to 25.8% methane and required 36 days of recovery (TWAS only influent) to return to its pre-shock level of 68.5% (Fig. 4E). Similar to the moderate shock comparison, these results show that, although both reactors still experienced upset, the effects were not as severe, indicating improved reactor robustness due to pre-exposure. This improved reactor robustness is likely due to changes in the microbial community structure that occurred during non-inhibitory FOG shock loads.

As observed with the methane content and productivity metrics discussed previously, the adapted and non-adapted C-shocks both exhibited similar levels of OA accumulation. The non-adapted reactor only showed a 9% increase in total OA accumulation compared to the adapted reactor (2.59 g/L and 2.38 g/L, respectively) (Fig. 4F). The non-adapted reactor had peak acetate, propionate, and butyrate concentrations of 1.62 g/L, 0.86 g/L, and 0.43 g/L, respectively while the adapted reactor reached peak concentrations of 1.54 g/L, 0.49 g/L, and 0.44 g/L, respectively (Figs. S1 and S3). These values were relatively similar, but the time to meet the recovery threshold was much greater for the non-adapted reactor which took 48.8 days of recovery (TWAS only influent) while the exposed reactor took only 31 days (Fig. 4F).

The pH of each respective reactor also exhibited this same phenomena. Throughout the majority of the shocks and recovery periods, the pH of the non-adapted reactor and the adapted reactor both stayed within the ideal pH range of 6.5–8 (Kundu et al., 2017). The adapted reactor experienced a low pH of 6.75 while the non-adapted reactor experienced a low of 6.32. Interestingly, the adapted reactor required only 34 days to recover its initial pH (TWAS only influent) while the non-adapted reactor required 53 days to do the same (Fig. 4G).

Quantification of the *mcrA* gene indicated that both reactors saw a similar decrease in methanogens following the shock event (Fig. 3H). Although the reactors did not start with the same concentration of methanogens, they both experienced decreases in methanogen abundance due to the shock event. The adapted reactor saw an 82% decrease in *mcrA* concentration while the non-adapted reactor saw a 96% decrease. The estimated recovery times were similar for both reactors where approximately 33 days of TWAS only influent was needed to return to pre-shock levels.

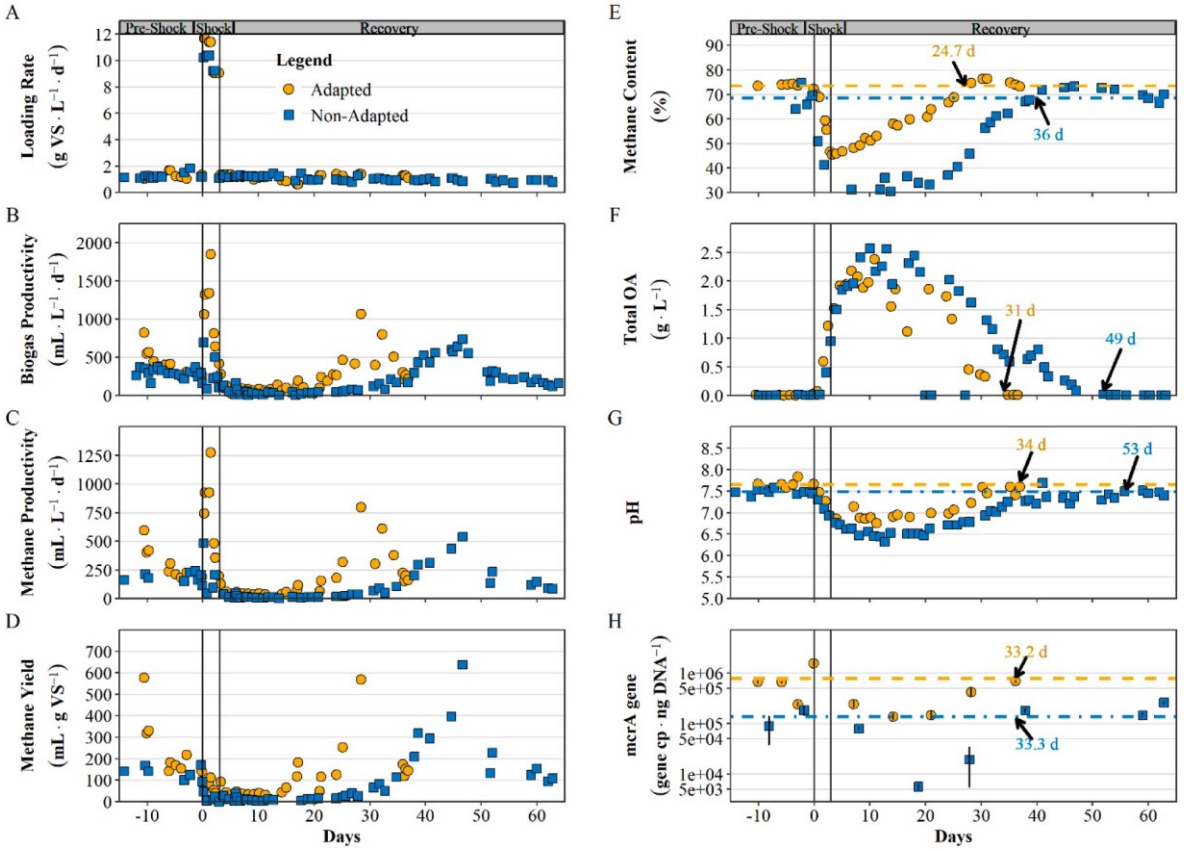

Fig. 4. A) Organic loading rate (OLR), B) biogas production, C) methane production, D) methane yield, E) methane content, F) total OA content, G) pH, and H) *mcrA* quantification for the adapted and non-adapted digesters during the pre-shock, moderate B-shock, and recovery phases. Dashed lines represent the pre-shock averages of each respective parameter. Arrows and labeled number of days represent how many days of TWAS only recovery was needed to reach pre-shock levels. Error bars on *mcrA* data represent 95% confidence intervals for triplicate samples.

To the best of the authors' knowledge, a shock load of this size has not been previously tested with FOG as the substrate. One study switched from mixed food waste to biodiesel to reach an OLR of 10 g COD/L/d for a short shock period of 5 days (Regueiro et al., 2015). The switch in substrate may have skewed the results in terms of reactor response to a change in substrate as well as an organic overload. Nonetheless, similar signs of reactor failure were observed when compared to the present study. At 10 g COD/L/d, biogas production decreased from approximately 3000 mL/L/d to 650 mL/L/d. The present study saw a more dramatic decrease in biogas production (from 318 to 30 mL/L/d) which is likely due to the pre-shock levels being lower than those in the Reguerio et al. study as they fed mixed food waste prior to the shock period. When considering OA accumulation caused by the rapid increase in OLR, Regueiro et al. saw OA concentrations up to 3 g/L of acetate and 6 g/L of propionate (Regueiro et al., 2015) which are more dramatic than those seen in the present study (1.62 g/L of acetate and 0.86 g/L of propionate). Although these results are different due to differences in substrate composition and feeding strategy, similar trends are observed in terms of reactor upset due to large, rapid increases in OLR indicating that adaptation will not be able to mitigate the effects of reactor failure during these types of overfeeding events.

3.3. Efficacy of repeated shock events for improving reactor resilience

3.3.1. Efficacy of repeated moderate shocks (B-shocks)

To determine if repeated exposure to moderate FOG shocks would increase robustness of the reactor even further, the adapted reactor was exposed to a series of three moderate B-shocks. The first repeated B-shocks (B1 –B3) did not illicit any signs of reactor upset, no decrease in gas production or methane content, and showed moderate OA accumulation (Fig. 5). However, an increase in reactor resilience, based on a decrease in OA accumulation, was observed with each subsequent shock (Fig. 5F). Peak acetate concentrations for B1, B2, and B3 were 0.93 g/L, 0.29 g/L, and 0.15 g/L, respectively, indicating that at a higher OLR, the microbial community was able to adapt further and effectively utilize FOG after successive periods of shock.

In contrast, this improvement in reactor resilience was not echoed in terms of methane productivity and yield (Fig. 5C and D). Of the three successive B-shocks, B1 exhibited the highest average productivity and yield on a biogas and specific methane basis. These results may be due to the large build-up of acetate observed during B1 which produced an inflated amount of biogas, and subsequently methane, toward the latter half of the phase. Other parameters measured such as pH and methane content were similar amongst all three B-shocks ranging from 7.48 to 7.91 and 67 to 74.2%, respectively (Fig. 5E and G). Quantification of the *mcrA* gene indicates that a similar concentration of methanogens was present at the beginning of each B-shock ranging from 2.81E4 to 1.51E5 (Fig. 5H). It also shows that B1 and B2 resulted in similar amounts of *mcrA* present after the shock, while B3 saw an 805% increase in abundance (8.55E4 to 7.74E5 gene copies/ng DNA). This further suggests that the successive B-shocks resulted in adaption of the microbial community to perform FOG co-digestion.

3.3.2. Efficacy of repeated large shocks (C-shocks)

To determine if repeated exposure to large FOG shocks would increase robustness of the reactor even further, the adapted reactor was exposed to a series of three large C-shocks. All three C-shocks, which had an OLR three times greater than the B-shocks, resulted in reactor upset and failure based on a rapid decrease in methane productivity, methane content, as well as a rapid accumulation of OAs due to the large organic load (Fig. 6). Repeated C-shocks did not improve reactor resistance and resilience to the same extent as seen with the repeated B-shocks.

Repeated failure-inducing C-shocks had an increasingly adverse effect on the reactor's resistance to failure. The lowest methane production rate was observed during the first shock event and the methane content values reached similar lows across all C-shocks with values of 45.4%, 49.9%, and 46% following C1, C2, and C3, respectively (Fig. 6E). In contrast, other parameters were more affected with each successive shock. The pH decreased more dramatically with each successive C-shock with minimum values of 6.85, 6.60, and 6.44 following C1, C2,

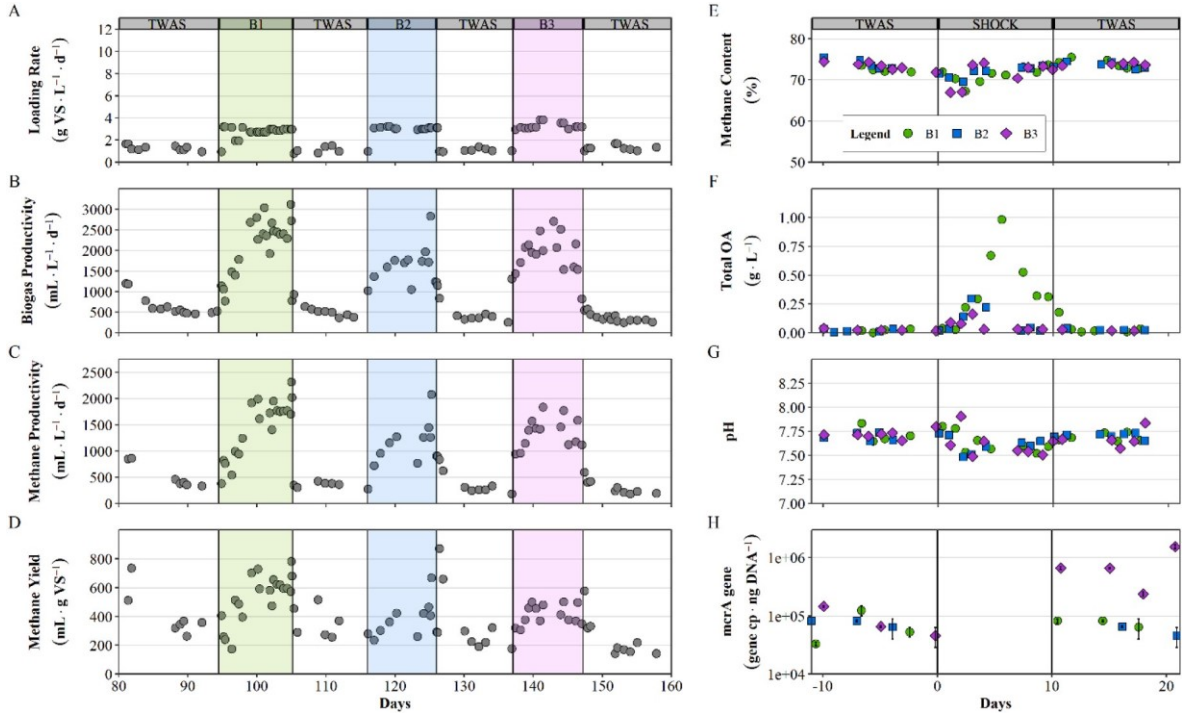

Fig. 5. A) Organic loading rate (OLR), B) biogas production, C) methane production, D) methane yield, E) methane content, F) total OA content, G) pH, and H) *mcrA* gene quantification for days 80–160 of the long-term experiment. Shocks B1, B2, and B3 are highlighted in green, blue, and purple, respectively. Black vertical lines designate the different phases of operation. Error bars on *mcrA* gene data represent 95% confidence intervals for triplicate samples.

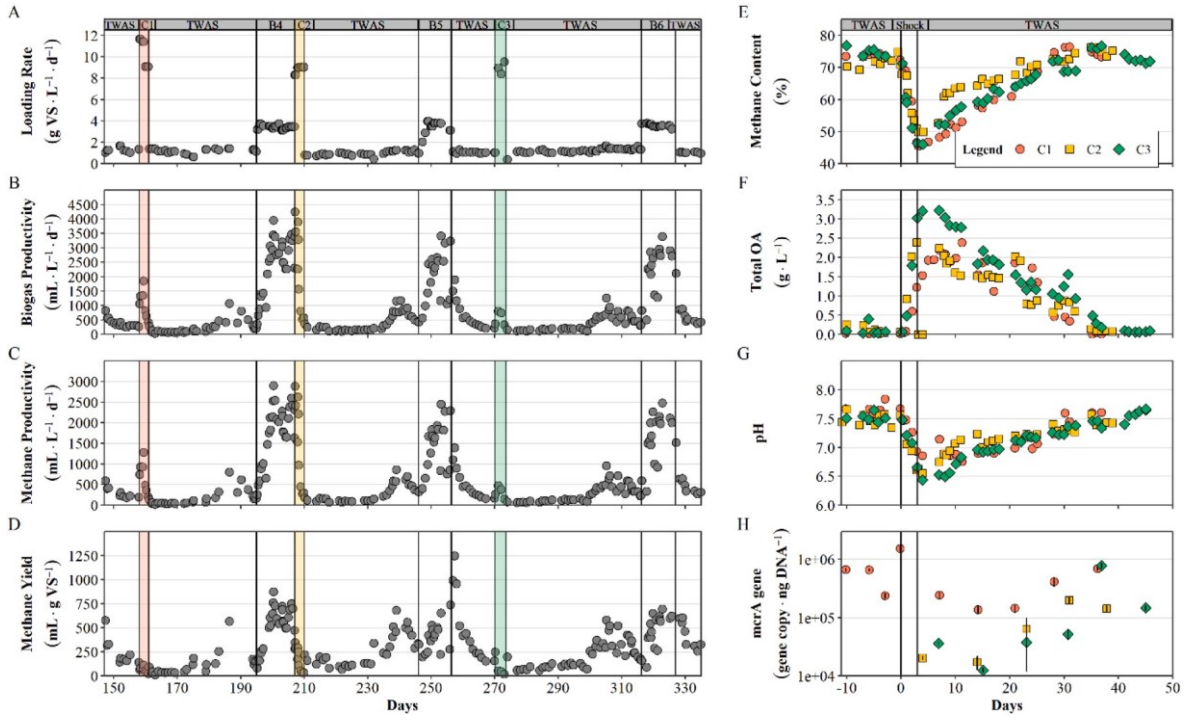

Fig. 6. A) Organic loading rate (OLR), B) biogas production, C) methane production, D) methane yield, E) methane content, F) total OA content, G) pH, and H) *mcrA* quantification for days 150–335 of the long-term experiment. Shocks C1, C2, and C3 are highlighted in red, yellow, and green, respectively. Black vertical lines designate the different phases of operation. Error bars on *mcrA* data represent 95% confidence intervals for triplicate samples.

and C3, respectively (Fig. 6G). The quantification of the *mcrA* gene also shows that each successive C-shock resulted in a greater decrease in methanogen abundance and a longer recovery time required (Fig. 6H). OA accumulation data also demonstrated increasingly adverse effects on reactor stability with each repeated C-shock (Fig. 6F). During C1, OA accumulation occurred rapidly and reached peak concentrations of acetate, propionate, and butyrate (1.54 g/L, 0.49 g/L, and 0.44 g/L, respectively) during the ensuing recovery phase. Shock C2 produced a similar response with similar peak concentrations of acetate, propionate, and butyrate (1.29 g/L, 0.48 g/L, and 0.36 g/L, respectively). The final C-shock, C3, resulted in increased peak concentrations of both acetate and propionate compared to the previous C-shocks, reaching 2 g/L of acetate and 0.98 g/L of propionate while the butyrate concentration reached 0.27 g/L. The amount of time it took for OA levels to fall below the established 50 mg/L threshold increased with each subsequent failure event as well. Shocks C1, C2, and C3 required 32 d, 36 d, and 40 d to recover (Fig. 6).

3.3.3. *Effects of repeated moderate and large shocks on reactor performance and resilience*

Following each C-shock and subsequent recovery period, an additional moderate B-shock was utilized to determine if the process upset had improved methane production and yields (Figs. 5 and 6). The first of these additional B-shocks, B4, achieved a similar methane yield to that of B1 ($p=0.901$) (Fig. 6). The average methane yield achieved during B4 was 626 $\pm$ 48 mL CH_4/g VS, which is greater than expected based on a similar study of co-digestion of primary solids and grease trap waste which saw a maximum methane yield of 463 mL CH_4/g VS (Luostarinen et al., 2009). However, there is substantial variability in the methane yields observed during the B-shocks with a slight increase in yield observed between pre-failure and post-failure averages, albeit not significantly.

In order to better understand this variability in methane yields in concert with the reactor's recovery following shock events, a resilience model proposed by Todman et al. was used to quantify the reactor resilience (Todman et al., 2016). The chosen parameters of interest are the time it took for the reactor to recover (return time) and the efficiency of the recovery period (Fig. 7).

Model results suggest that there is a trade-off between reactor stability in terms of resistance to signs of upset and improved performance in terms of methane production and yield (Fig. 7). The return time and efficiency for the first three B-shocks (B1–B3) show improvement (decrease in return time and decrease in efficiency) with each subsequent shock. However, the latter B shocks (B4–B6) don't follow the same trend and are not as optimized as B3, suggesting that the failure inducing shocks (C1–C3) effectively erased any positive shifts in the microbial community produced during shocks B1–B3. The unique conditions created by these failure events likely induce either a reseeding of the microbial community or a shift to an entirely different community structure.

Similarly, with each subsequent C-shock the return time and efficiency increased, indicating that the microbial community was becoming more sensitive to the failure events over time. Again, with each subsequent failure event, the microbial community must adapt to and recover from the unique conditions created by each failure event that occurred. This trend was also seen in the return time and efficiency values for the methane content.

Conversely, the methane content results don't follow the same trend as the OA accumulation results for the B-shocks. There was neither improvement nor deterioration of the return time or efficiency for all six B-shocks, indicating that the increased stability observed during B1–B3 is not echoed in terms of methane productivity. This further suggests that the archaeal community responsible for methane production are more difficult to mold with pulse disturbances compared to their bacterial counterparts which are responsible for OA degradation. This is likely due to greater functional redundancy often observed in the bacterial community present in anaerobic digesters compared to archaeal communities (Paulo et al., 2020).

Other loading regime studies have not studied the effects of pulse disturbances with FOG making it difficult to directly compare reactor

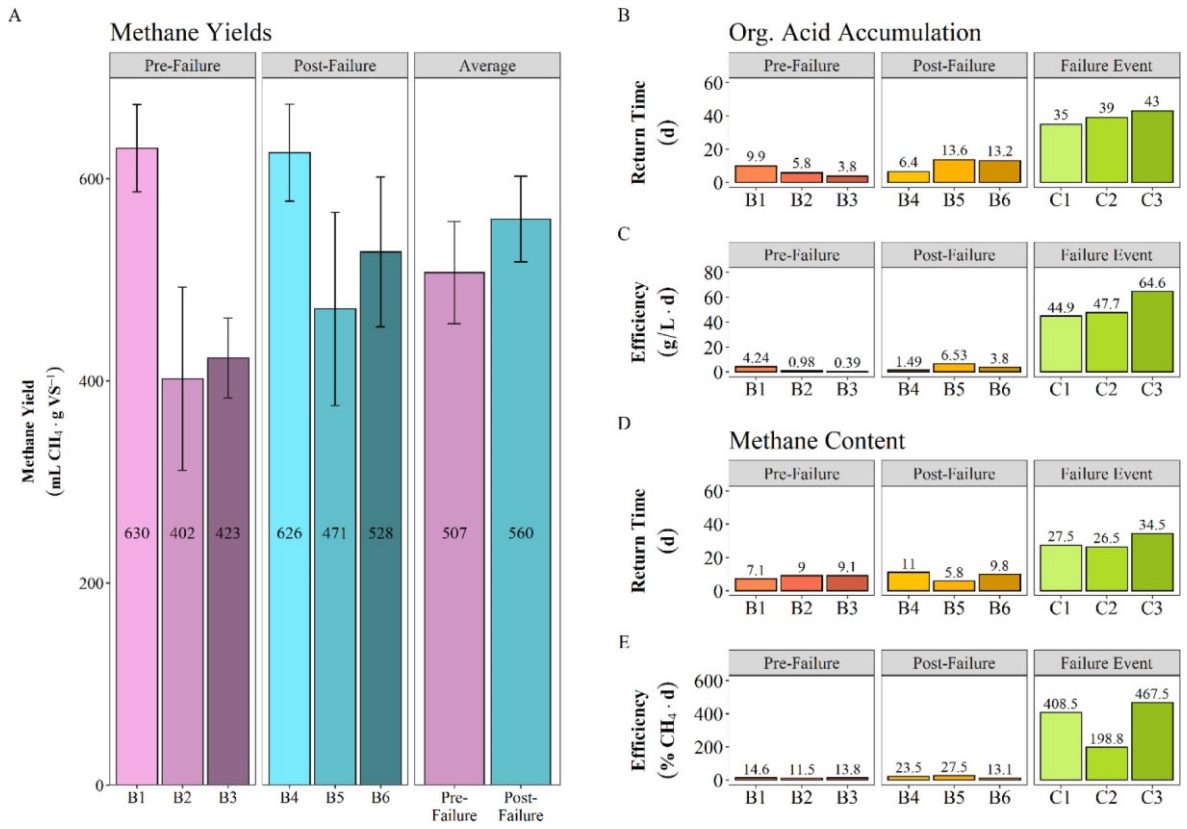

Fig. 7. A) Methane yields for each B-shock administered throughout the duration of the long-term experiment. For each individual shock, averages were taken over days 3–10 of the shock event. Error bars represent 95% confidence intervals. B-E) Model results derived from the adaptation of the resilience model proposed by Todman et al. (Todman et al., 2016). Parameters shown are return time and return efficiency for both the OA accumulation data (B and C) as well as the methane content data (D and E).

responses during a disturbance-to-failure event. However, it has been previously observed that when the OLR was increased to values of 1.7–4.4 g VS/L/d, the methane yield did not increase and no signs of inhibition were observed, although there were increases in residual LCFAs and OAs (Luostarinen et al., 2009; Silvestre et al., 2011). Similarly, Wang et al. observed that extended FOG press disturbances (20–80 days long), at a maximum OLR of approximately 3.2 g VS/L/d (similar to the moderate shock loads of this study), resulted in increased methane yields but led to increased instability when the reactors were re-stressed (Wang et al., 2020). Thus, these previous studies are in-line with the model results of thie present study, which indicates a trade-off between improved performance and improved resistance to upset.

4. Conclusions

Pre-exposure to small and moderate FOG shock loads resulted in avoidance of reactor upset at moderate shock loads and mitigation of the effects of reactor upset at large shock loads. However, methane yield was not improved. Repeated large shocks resulted in disturbance-to-failure events that also did not improve methane yield and decreased the anaerobic digester's resistance and resilience to future large shock loads. Thus, this work demonstrates that there is a tipping point in which FOG shock loads, whether intentional or accidental, go from improving the overall robustness of an anaerobic digester to significantly deteriorating its overall performance. A further study of the microbial community dynamics during these FOG shock loads could assist in efforts to further understand the effects of shock loads on the anaerobic co-digestion of FOG.

CRediT authorship contribution statement

Ashley E. Berninghaus: Conceptualization, Methodology, Visualization, Writing – original draft, Writing – review & editing, Experimentation, Data Collection, Interpretation, Data Visualization, Writing – original manuscript and editing. **Tyler S. Radniecki:** Conceptualization, Interpretation, Supervision, Funding acquisition, Writing – review & editing.

Declaration of competing interest

The authors declare that they have no known competing financial interests or personal relationships that could have appeared to influence the work reported in this paper.

Acknowledgments

This study was supported by the NSF CAREER Grant #1847654. The authors would like to thank the individuals who aided in reactor maintenance and data collection efforts: Lindsay Benage, Jackson Schleicher, and Ross Warner. The authors are especially grateful to the staff of the City of Corvallis Wastewater Reclamation Plant for their assistance with sample collection as well as the staff at Jacobs Engineering Inc. who run the City of Gresham Wastewater Reclamation Plant for their assistance with FOG collection.

Appendix A. Supplementary data

Supplementary data to this article can be found online at https://doi.org/10.1016/j.jclepro.2022.132447.

References

Carballa, M., Regueiro, L., Lema, J.M., 2015. Microbial management of anaerobic digestion: exploiting the microbiome-functionality nexus. Curr. Opin. Biotechnol. 33, 103–111.

Davidsson, Å., Lo¨vstedt, C., la Cour Jansen, J., Gruvberger, C., Aspegren, H., 2008. Co-digestion of grease trap sludge and sewage sludge. Waste Manag. 28 (6), 986–992.

Deaver, J.A., Soni, M.N., Diviesti, K.I., Finneran, K.T., Shankar, V., Popat, S.C., 2021. Taxonomic and functional variations induced by an overloading event in anaerobic codigestion of municipal wastewater sludge with fats, oils, and grease. ACS ES&T Eng. 1 (8), 1205–1216.

Goux, X., Calusinska, M., Lemaigre, S., Marynowska, M., Klocke, M., Udelhoven, T., Benizri, E., Delfosse, P., 2015. Microbial community dynamics in replicate anaerobic digesters exposed sequentially to increasing organic loading rate, acidosis, and process recovery. Biotechnol. Biofuels 8 (1), 122.

Grosser, A., Neczaj, E., 2018. Sewage sludge and fat rich materials co-digestion - performance and energy potential. J. Clean. Prod. 198, 1076–1089.

Kabouris, J.C., Tezel, U., Pavlostathis, S.G., Engelmann, M., Todd, A.C., Gillette, R.A., 2008. The anaerobic biodegradability of municipal sludge and fat, oil, and grease at mesophilic conditions. Water Environ. Res. 80 (3), 212–221.

Kougias, P.G., Treu, L., Campanaro, S., Zhu, X., Angelidaki, I., 2016. Dynamic functional characterization and phylogenetic changes due to Long Chain Fatty Acids pulses in biogas reactors. Sci. Rep. 6 (1), 28810.

Kundu, K., Sharma, S., Sreekrishnan, T.R., 2017. Influence of process parameters on anaerobic digestion microbiome in bioenergy production: towards an improved understanding. BioEnergy Res. 10 (1), 288–303.

Lee, U., Bhatt, A., Hawkins, T.R., Tao, L., Benavides, P.T., Wang, M., 2021. Life cycle analysis of renewable natural gas and lactic acid production from waste feedstocks. J. Clean. Prod. 311, 127653.

Li, C., Champagne, P., Anderson, B.C., 2013. Biogas production performance of mesophilic and thermophilic anaerobic co-digestion with fat, oil, and grease in semi-continuous flow digesters: effects of temperature, hydraulic retention time, and organic loading rate. Environ. Technol. 34 (13–14), 2125–2133.

Long, J.H., Aziz, T.N., Reyes, F.L.d.l., Ducoste, J.J., 2012. Anaerobic co-digestion of fat, oil, and grease (FOG): a review of gas production and process limitations. Process Saf. Environ. Protect. 90 (3), 231–245.

Luostarinen, S., Luste, S., Sillanp¨a¨a, M., 2009. Increased biogas production at wastewater treatment plants through co-digestion of sewage sludge with grease trap sludge from a meat processing plant. Bioresour. Technol. 100 (1), 79–85.

Luton, P.E., Wayne, J.M., Sharp, R.J., Riley, P.W., 2002. The mcrA gene as an alternative to 16S rRNA in the phylogenetic analysis of methanogen populations in landfillbbThe GenBank accession numbers for the mcrA sequences reported in this paper are AF414034–AF414051 (see Fig. 2) and AF414007–AF414033 (environmental isolates in Fig. 3). Microbiology 148 (11), 3521–3530.

Morris, R., Schauer-Gimenez, A., Bhattad, U., Kearney, C., Struble, C.A., Zitomer, D., Maki, J.S., 2014. Methyl coenzyme M reductase (mcrA) gene abundance correlates with activity measurements of methanogenic H_2/CO_2 -enriched anaerobic biomass. Microb. Biotechnol. 7 (1), 77–84.

Parry, D., 2010. Co-Digestino of Organic Waste Products with Wastewater Solids. WERF.

Paulo, L.M., Castilla-Archilla, J., Ramiro-Garcia, J., Escamez-Pico´n, J.A., Hughes, D., Mahony, T., Murray, M., Wilmes, P., O'Flaherty, V., 2020. Microbial community redundancy and resilience underpins high-rate anaerobic treatment of dairy-processing wastewater at ambient temperatures. Front. Bioeng. Biotechnol. 8, 192.

Regueiro, L., Lema, J.M., Carballa, M., 2015. Key microbial communities steering the functioning of anaerobic digesters during hydraulic and organic overloading shocks. Bioresour. Technol. 197, 208–216.

Rhine, E.D., Sims, G.K., Mulvaney, R.L., Pratt, E.J., 1998. Improving the Berthelot reaction for determining ammonium in soil extracts and water. Soil Sci. Soc. Am. J. 62 (2), 473–480.

Salama, E.-S., Saha, S., Kurade, M.B., Dev, S., Chang, S.W., Jeon, B.-H., 2019. Recent trends in anaerobic co-digestion: fat, oil, and grease (FOG) for enhanced biomethanation. Prog. Energy Combust. Sci. 70, 22–42.

Shade, A., Peter, H., Allison, S.D., Baho, D.L., Berga, M., Bürgmann, H., Huber, D.H., Langenheder, S., Lennon, J.T., Martiny, J.B.H., Matulich, K.L., Schmidt, T.M., Handelsman, J., 2012. Fundamentals of microbial community resistance and resilience. Front. Microbiol. 3, 417.

Silvestre, G., Rodríguez-Abalde, A., Ferna´ndez, B., Flotats, X., Bonmatí, A., 2011. Biomass adaptation over anaerobic co-digestion of sewage sludge and trapped grease waste. Bioresour. Technol. 102 (13), 6830–6836.

Suto, P., Gray, D., Larsen, E., Hake, J., 2006. Innovative anaerobic digestion investigatin of fats, oils, and grease. In: Residuals and Biosolids Management Conference. Water Environment Federation, pp. 858–879.

Todman, L.C., Fraser, F.C., Corstanje, R., Deeks, L.K., Harris, J.A., Pawlett, M., Ritz, K., Whitmore, A.P., 2016. Defining and quantifying the resilience of responses to disturbance: a conceptual and modelling approach from soil science. Sci. Rep. 6 (1), 28426.

U.S. EPA, 1978. Method 365.3: Phosphorous, All Forms (Colorimetric, Ascorbic Acid, Two Reagent).

U.S. EPA, Office of Water, 2001. Method 1684: Total, Fixed, and Volatile Solids in Water, Solids, and Biosolids.

Wang, H., Zhang, Y., Angelidaki, I., 2016. Ammonia inhibition on hydrogen enriched anaerobic digestion of manure under mesophilic and thermophilic conditions. Water Res. 105, 314–319.

Wang, L., Hossen, E.H., Aziz, T.N., Ducoste, J.J., de los Reyes, F.L., 2020. Increased loading stress leads to convergence of microbial communities and high methane yields in adapted anaerobic co-digesters. Water Res. 169, 115155.

Yenigun, O., Demirel, B., 2013. Ammonia inhibition in anaerobic digestion: a review. Process Biochem. 48 (5–6), 901–911.

Ziels, R.M., Beck, D.A.C., Stensel, H.D., 2017. Long-chain fatty acid feeding frequency in anaerobic codigestion impacts syntrophic community structure and biokinetics. Water Res. 117, 218–229.

Ziels, R.M., Karlsson, A., Beck, D.A.C., Ejlertsson, J., Yekta, S.S., Bjorn, A., Stensel, H.D., Svensson, B.H., 2016. Microbial community adaptation influences long-chain fatty acid conversion during anaerobic codigestion of fats, oils, and grease with municipal sludge. Water Res. 103, 372–382.